Quantum Monte Carlo diagonalization for many-fermion systems

Takashi Yanagisawa
Condensed-Matter Physics Group, Nanoelectronics Research Institute, AIST Central 2, 1-1-1 Umezono, Tsukuba 305-8568, Japan and CREST, Japan Science and Technology Agency (JST), Kawaguchi-shi, Saitama 332-0012, Japan
(Received 23 August 2006; revised manuscript received 16 January 2007; published 6 June 2007)

In this study we present an optimization method based on the quantum Monte Carlo diagonalization for many-fermion systems. Using the Hubbard-Stratonovich transformation, employed to decompose the interactions in terms of auxiliary fields, we expand the true ground-state wave function. The ground-state wave function is written as a linear combination of the basis wave functions. The Hamiltonian is diagonalized to obtain the lowest energy state using the variational principle within the selected subspace of the basis functions. This method is free from the difficulty known as *the negative sign problem*. We can optimize a wave function using two procedures. The first procedure is to increase the number of basis functions. The second improves each basis function through the operators $e^{-\Delta\tau H}$ using the Hubbard-Stratonovich decomposition. We present an algorithm for the quantum Monte Carlo diagonalization method using a genetic algorithm and the renormalization method. We compute the ground-state energy and correlation functions of small clusters to compare with available data.

DOI: 10.1103/PhysRevB.75.224503 PACS number(s): 74.20.−z, 71.10.Fd, 75.40.Mg

I. INTRODUCTION

The effect of the strong correlation between electrons is important for many quantum critical phenomena, such as unconventional superconductivity and the metal-insulator transition. Typical correlated electron systems are high-temperature superconductors,[1–4] heavy fermions,[5–8] and organic conductors.[9] Recently, the mechanisms of superconductivity in high-temperature superconductors and organic superconductors have been extensively studied using various two-dimensional (2D) models of electronic interactions. Among them, the 2D Hubbard model[10] is the simplest and most fundamental model. This model has been studied intensively using numerical tools, such as the quantum Monte Carlo method[11–24] and the variational Monte Carlo method.[25–33] Recently, the two-leg ladder Hubbard model was also investigated with respect to the mechanism of high-temperature superconductivity.[34–41]

The quantum Monte Carlo (QMC) method is a numerical method employed to simulate the behavior of correlated electron systems. It is well known, however, that there are significant issues associated with the application to the QMC. First, the standard Metropolis (or heat bath) algorithm is associated with the negative sign problem. Second, the convergence of the trial wave function is sometimes not monotonic, and further, is sometimes slow. In past studies, workers have investigated the possibility of eliminating the negative sign problem.[21,22,24] If the negative sign problem can be eliminated, the next task would be to improve the convergence of the simulation method.

In this paper, we present an optimization method based on quantum Monte Carlo diagonalization (QMD). The recent developments of high-performance computers have led to the possibility of the simulation of correlated electron systems using diagonalization. Typically, and as in this study, the ground-state wave function is defined as

$$\psi = e^{-\tau H}\psi_0, \tag{1.1}$$

where H is the Hamiltonian and ψ_0 is the initial one-particle state such as the Fermi sea. In the QMD method, this wave function is written as a linear combination of the basis states, generated using the auxiliary field method based on the Hubbard-Stratonovich transformation; that is,

$$\psi = \sum_m c_m \phi_m, \tag{1.2}$$

where ϕ_m are basis functions. In this work, we have assumed a subspace with N_{states} basis wave functions. From the variational principle, the coefficients $\{c_m\}$ are determined from the diagonalization of the Hamiltonian to obtain the lowest energy state in the selected subspace $\{\phi_m\}$. Once the c_m coefficients are determined, the ground-state energy and other quantities are calculated using this wave function. If the expectation values are not highly sensitive to the number of basis states, we can obtain the correct expectation values using an extrapolation in terms of the basis states at the limit $N_{states}\rightarrow\infty$. However, a more reliable procedure must be employed when the change in the values at the limit is not monotonic. In this study, results are compared to results obtained from an exact diagonalization of small clusters, such as 4×4 and 6×2 lattices.

In the following section, Sec. II, we briefly review the standard quantum Monte Carlo simulation approach. In Sec. III, a discussion of the quantum Monte Carlo diagonalization and an extrapolation method to obtain the expectation values are presented. Section IV is a discussion of the optimization procedure which employs the diagonalization method. All the results obtained in this study are compared to the exact and available results of small systems in Sec. V. Finally, a summary of the work presented in this paper is presented in Sec. VI.

II. QUANTUM MONTE CARLO METHOD

The method of quantum Monte Carlo diagonalization lies in the QMC method. Thus it is appropriate to first outline the QMC method. The Hamiltonian is the Hubbard model con-

taining on-site Coulomb repulsion and is written as

$$H = -\sum_{ij\sigma} t_{ij}(c_{i\sigma}^{\dagger}c_{j\sigma} + \text{H.c.}) + U\sum_{j} n_{j\uparrow}n_{j\downarrow}, \tag{2.1}$$

where $c_{j\sigma}^{\dagger}$ ($c_{j\sigma}$) is the creation (annihilation) operator of an electron with spin σ at the jth site and $n_{j\sigma}=c_{j\sigma}^{\dagger}c_{j\sigma}$. t_{ij} is the transfer energy between the sites i and j. $t_{ij}=t$ for the nearest-neighbor bonds. For all other cases, $t_{ij}=0$. U is the on-site Coulomb energy. The number of sites is N and the linear dimension of the system is denoted as L. The energy unit is given by t and the number of electrons is denoted as N_e.

In a quantum Monte Carlo simulation, the ground-state wave function is

$$\psi = e^{-\tau H}\psi_0, \tag{2.2}$$

where ψ_0 is the initial one-particle state represented by a Slater determinant. For large τ, $e^{-\tau H}$ will project out the ground-state from ψ_0. We write the Hamiltonian as $H=K+V$, where K and V are the kinetic and interaction terms of the Hamiltonian in Eq. (2.1), respectively. The wave function in Eq. (2.2) is written as

$$\psi = (e^{-\Delta\tau(K+V)})^M\psi_0 \approx (e^{-\Delta\tau K}e^{-\Delta\tau V})^M\psi_0, \tag{2.3}$$

for $\tau=\Delta\tau\cdot M$. Using the Hubbard-Stratonovich transformation,[11,42] we have

$$\exp(-\Delta\tau U n_{i\uparrow}n_{i\downarrow}) = \frac{1}{2}\sum_{s_i=\pm 1}\exp\left[2as_i(n_{i\uparrow}-n_{i\downarrow}) - \frac{1}{2}U\Delta\tau(n_{i\uparrow}+n_{i\downarrow})\right], \tag{2.4}$$

for $(\tanh a)^2=\tanh(\Delta\tau U/4)$ or $\cosh(2a)=e^{\Delta\tau U/2}$. The wave function is expressed as a summation of the one-particle Slater determinants over all the configurations of the auxiliary fields $s_j=\pm 1$. The exponential operator is expressed as

$$(e^{-\Delta\tau K}e^{-\Delta\tau V})^M = \frac{1}{2^{NM}}\sum_{\{s_i(\ell)\}}\prod_{\sigma} B_M^{\sigma}(s_i(M)) \times B_{M-1}^{\sigma}(s_i(M-1))\cdots B_1^{\sigma}(s_i(1)), \tag{2.5}$$

where we have defined

$$B_{\ell}^{\sigma}(\{s_i(\ell)\}) = e^{-\Delta\tau K_{\sigma}}e^{-V_{\sigma}(\{s_i(\ell)\})} \tag{2.6}$$

for

$$V_{\sigma}(\{s_i\}) = 2a\sigma\sum_i s_i n_{i\sigma} - \frac{1}{2}U\Delta\tau\sum_i n_{i\sigma}, \tag{2.7}$$

$$K_{\sigma} = -\sum_{ij} t_{ij}(c_{i\sigma}^{\dagger}c_{j\sigma} + \text{H.c.}). \tag{2.8}$$

The ground-state wave function is

$$\psi = \sum_m c_m\phi_m, \tag{2.9}$$

where ϕ_m is a Slater determinant corresponding to a configuration $m=\{s_i(\ell)\}$ $(i=1,\ldots,N;\ell=1,\ldots,M)$ of the auxiliary fields:

$$\phi_m = \prod_{\sigma} B_M^{\sigma}(s_i(M))\cdots B_1^{\sigma}(s_i(1))\psi_0 \equiv \phi_m^{\uparrow}\phi_m^{\downarrow}. \tag{2.10}$$

The coefficients c_m are constant real numbers: $c_1=c_2=\ldots$. The initial state ψ_0 is a one-particle state. If electrons occupy the wave numbers $k_1,k_2,\ldots,k_{N_{\sigma}}$ for each spin σ, ψ_0 is given by the product $\psi_0^{\uparrow}\psi_0^{\downarrow}$, where ψ_0^{σ} is the matrix represented as[15]

$$\begin{pmatrix} e^{ik_1\cdot r_1} & e^{ik_2\cdot r_1} & \cdots & \cdots & e^{ik_{N_{\sigma}}\cdot r_1} \\ e^{ik_1\cdot r_2} & e^{ik_2\cdot r_2} & \cdots & \cdots & \cdots \\ \vdots & \vdots & \vdots & \vdots & \vdots \\ e^{ik_1\cdot r_N} & e^{ik_2\cdot r_N} & \cdots & \cdots & \end{pmatrix}. \tag{2.11}$$

N_{σ} is the number of electrons for spin σ. In actual calculations, we can use a real representation where the matrix elements are $\cos(k_i\cdot r_j)$ or $\sin(k_i\cdot r_j)$. In the real-space representation, the matrix of $V_{\sigma}(\{s_i\})$ is a diagonal matrix given as

$$V_{\sigma}(\{s_i\}) = \text{diag}(2a\sigma s_1 - U\Delta\tau/2,\ldots,2a\sigma s_N - U\Delta\tau/2). \tag{2.12}$$

The matrix elements of K_{σ} are

$$(K_{\sigma})_{ij} = -t, \quad i,j \text{ are nearest neighbors}$$
$$= 0 \quad \text{otherwise}. \tag{2.13}$$

ϕ_m^{σ} is an $N\times N_{\sigma}$ matrix given by the product of the matrices $e^{-\Delta\tau K_{\sigma}}$, $e^{V_{\sigma}}$, and ψ_0^{σ}. The inner product is thereby calculated as a determinant,[22]

$$\langle\phi_m^{\sigma}\phi_n^{\sigma}\rangle = \det(\phi_m^{\sigma\dagger}\phi_n^{\sigma}). \tag{2.14}$$

The expectation value of the quantity Q is evaluated as

$$\langle Q\rangle = \frac{\sum_{mn}\langle\phi_m Q\phi_n\rangle}{\sum_{mn}\langle\phi_m\phi_n\rangle}. \tag{2.15}$$

If Q is a bilinear operator Q_{σ} for spin σ, we have

$$\langle Q_{\sigma}\rangle = \frac{\sum_{mn}\langle\phi_m^{\sigma}Q_{\sigma}\phi_n^{\sigma}\rangle\langle\phi_m^{-\sigma}\phi_n^{-\sigma}\rangle}{\sum_{mn}\langle\phi_m^{\sigma}\phi_n^{\sigma}\rangle\langle\phi_m^{-\sigma}\phi_n^{-\sigma}\rangle} = \frac{\sum_{mn}\langle\phi_m^{\sigma}Q_{\sigma}\phi_n^{\sigma}\rangle\det(\phi_m^{-\sigma\dagger}\phi_n^{-\sigma})}{\sum_{mn}\det(\phi_m^{\sigma\dagger}\phi_n^{\sigma})\det(\phi_m^{-\sigma\dagger}\phi_n^{-\sigma})} = \sum_{mn}\frac{\det(\phi_m^{\sigma\dagger}\phi_n^{\sigma})\det(\phi_m^{-\sigma\dagger}\phi_n^{-\sigma})}{\sum_{m'n'}\det(\phi_{m'}^{\sigma\dagger}\phi_{n'}^{\sigma})\det(\phi_{m'}^{-\sigma\dagger}\phi_{n'}^{-\sigma})}\frac{\langle\phi_m^{\sigma}Q_{\sigma}\phi_n^{\sigma}\rangle}{\langle\phi_m^{\sigma}\phi_n^{\sigma}\rangle}. \tag{2.16}$$

The expectation value with respect to the Slater determinants $\langle\phi_m^{\sigma}Q_{\sigma}\phi_n^{\sigma}\rangle$ is evaluated using the single-particle Green's function,[15,22]

$$\frac{\langle \phi_m^\sigma c_{i\sigma} c_{j\sigma}^\dagger \phi_n^\sigma \rangle}{\langle \phi_m^\sigma \phi_n^\sigma \rangle} = \delta_{ij} - [\phi_n^\sigma (\phi_m^{\sigma\dagger} \phi_n^\sigma)^{-1} \phi_m^{\sigma\dagger}]_{ij}. \quad (2.17)$$

In the above expression, $P_{mn} \equiv \det(\phi_m^\sigma \phi_n^\sigma)\det(\phi_m^{-\sigma} \phi_n^{-\sigma})$ can be regarded as the weighting factor to obtain the Monte Carlo samples. Since this quantity is not necessarily positive definite, the weighting factor should be $|P_{mn}|$; the resulting relationship is

$$\langle Q_\sigma \rangle = \frac{\sum_{mn} P_{mn} \langle Q_\sigma \rangle_{mn}}{\sum_{mn} P_{mn}} = \frac{\sum_{mn} |P_{mn}| \mathrm{sign}(P_{mn}) \langle Q_\sigma \rangle_{mn}}{\sum_{mn} |P_{mn}| \mathrm{sign}(P_{mn})}, \quad (2.18)$$

where $\mathrm{sign}(a) = a/|a|$ and

$$\langle Q_\sigma \rangle_{mn} = \frac{\langle \phi_m^\sigma Q_\sigma \phi_n^\sigma \rangle}{\langle \phi_m^\sigma \phi_n^\sigma \rangle}. \quad (2.19)$$

This relation can be evaluated using a Monte Carlo procedure if an appropriate algorithm, such as the Metropolis or heat bath method, is employed.[42] The summation can be evaluated using appropriately defined Monte Carlo samples,

$$\langle Q_\sigma \rangle = \frac{\frac{1}{n_{MC}} \sum_{mn} \mathrm{sign}(P_{mn}) \langle Q_\sigma \rangle_{mn}}{\frac{1}{n_{MC}} \sum_{mn} \mathrm{sign}(P_{mn})}, \quad (2.20)$$

where n_{MC} is the number of samples. The sign problem is an issue if the summation of $\mathrm{sign}(P_{mn})$ vanishes within statistical errors. In this case, it is indeed impossible to obtain definite expectation values.

III. QUANTUM MONTE CARLO DIAGONALIZATION

A. Diagonalization

QMD is a method for the evaluation of $\langle Q_\sigma \rangle$ without *the negative sign problem*. The configuration space of the probability $|P_{mn}|$ in Eq. (2.20) is generally very strongly peaked. The sign problem lies in the distribution of P_{mn} in the configuration space. It is important to note that the distribution of the basis functions ϕ_m $(m=1,2,\ldots)$ is uniform since c_m are constant numbers: $c_1=c_2=\ldots$. In the subspace $\{\phi_m\}$, selected from all configurations of auxiliary fields, the right-hand side of Eq. (2.15) can be determined. However, the large number of basis states required to obtain accurate expectation values is beyond the current storage capacity of computers. Thus we use the variational principle to obtain the expectation values.

From the variational principle,

$$\langle Q \rangle = \frac{\sum_{mn} c_m c_n \langle \phi_m Q \phi_n \rangle}{\sum_{mn} c_m c_n \langle \phi_m \phi_n \rangle}, \quad (3.1)$$

where c_m $(m=1,2,\ldots)$ are variational parameters. In order to minimize the energy

$$E = \frac{\sum_{mn} c_m c_n \langle \phi_m H \phi_n \rangle}{\sum_{mn} c_m c_n \langle \phi_m \phi_n \rangle}, \quad (3.2)$$

the equation $\partial E/\partial c_n = 0$ $(n=1,2,\ldots)$ is solved for

$$\sum_m c_m \langle \phi_n H \phi_m \rangle - E \sum_m c_m \langle \phi_n \phi_m \rangle = 0. \quad (3.3)$$

If we set

$$H_{mn} = \langle \phi_m H \phi_n \rangle, \quad (3.4)$$

$$A_{mn} = \langle \phi_m \phi_n \rangle, \quad (3.5)$$

the eigenequation is

$$Hu = EAu \quad (3.6)$$

for $u=(c_1,c_2,\ldots)^t$. Since ϕ_m $(m=1,2,\ldots)$ are not necessarily orthogonal, A is not a diagonal matrix. We diagonalize the Hamiltonian $A^{-1}H$, and then calculate the expectation values of correlation functions with the ground-state eigenvector; in general, $A^{-1}H$ is not a symmetric matrix.

In order to optimize the wave function, we must increase the number of basis states $\{\phi_m\}$. This can be simply accomplished through random sampling. For systems of small sizes and small U, we can evaluate the expectation values from an extrapolation of the basis of randomly generated states.

B. Extrapolation

In quantum Monte Carlo simulations, an extrapolation is performed to obtain the expectation values for the ground-state wave function. If M is large enough, the wave function in Eq. (2.9) will approach the exact ground-state wave function, ψ_{exact}, as the number of basis functions, N_{states}, is increased. If the number of basis functions is large enough, the wave function will approach ψ_{exact} as M is increased. In either case, the method employed for the reliable extrapolation of the wave function is a key issue in calculating the expectation values. If the convergence is fast enough, the expectation values can be obtained from the extrapolation in terms of $1/N_{states}$. Note that although the extrapolation in terms of $1/M$, or the time step $\Delta\tau$, has often been employed in QMC calculations, however, a linear dependence for $1/M$ or $\Delta\tau$ will not necessarily guarantee an accurate extrapolated result. The variance method was recently proposed in variational and quantum Monte Carlo simulations, where the extrapolation is performed as a function of the variance. An advantage of the variance method lies in the fact that linearity is expected in some cases:[24,43]

$$\langle Q \rangle - Q_{exact} \propto v, \quad (3.7)$$

where v denotes the variance defined as

$$v = \frac{\langle (H - \langle H \rangle)^2 \rangle}{\langle H \rangle^2} \quad (3.8)$$

and Q_{exact} is the expected exact value of the quantity Q.

The following brief proof clearly shows that the energy in Eq. (3.8) varies linearly. If we denote the exact ground-state

wave function as ψ_g and the excited states as ψ_i ($i=1,2,\ldots$), the wave function can be written as

$$\psi = a\psi_g + \sum_i b_i \psi_i, \tag{3.9}$$

where we assume that a and b_i are real and satisfy $a^2+\Sigma_i b_i^2=1$. If it is assumed that $H\psi_g=E_g\psi_g$ and $H\psi_i=E_i\psi_i$, the energy is found to be

$$E=\langle H\rangle = a^2\langle\psi_g H\psi_g\rangle + 2a\sum_i b_i\langle\psi_i H\psi_g\rangle + \sum_{ij} b_i b_j\langle\psi_i H\psi_j\rangle$$
$$= a^2 E_g + \sum_{ij} b_i b_j\langle\psi_i H\psi_j\rangle = a^2 E_g + \sum_i b_i^2 E_i. \tag{3.10}$$

The deviation of E from E_g is

$$\delta E = E - E_g = (a^2-1)E_g + \sum_i b_i^2 E_i = b^2(\langle E_i\rangle - E_g), \tag{3.11}$$

where $b^2=1-a^2$ and $\langle E_i\rangle=\Sigma_j b_j^2 E_j/\Sigma_j b_j^2$. The variance v of H is also shown to be proportional to b^2 if b^2 is small. Since $\langle H^2\rangle=a^2E_g+b^2\langle E_i^2\rangle$, where $\langle E_i^2\rangle=\Sigma_j b_j^2 E_j^2/\Sigma_j b_j^2$, v is evaluated as

$$v = C\left\{(1-b^2)\frac{\delta E}{E_g} - 2\left(\frac{\delta E}{E_g}\right)^2 + \ldots\right\} \tag{3.12}$$

for a constant C. Hence if b is small, it is found that

$$\frac{\delta E}{E_g} = \frac{v}{C} + O(v^2). \tag{3.13}$$

The other quantities can be found if $Q_g=\langle\psi_g Q\psi_g\rangle$, which leads to the result

$$\langle Q\rangle - Q_g = -b^2 Q_g + 2a\sum_i b_i\langle\psi_i Q\psi_g\rangle + \sum_{ij} b_i b_j\langle\psi_i Q\psi_j\rangle. \tag{3.14}$$

If Q commutes with H, and ψ_i are eigenstates of Q, $\langle Q\rangle - Q_g$ is proportional to b^2:

$$\langle Q\rangle - Q_g = -b^2(Q_g - \langle Q_i\rangle), \tag{3.15}$$

where $\langle Q_i\rangle=\Sigma_i b_i^2\langle\psi_i Q\psi_i\rangle/\Sigma_i b_i^2$; thus $\langle Q\rangle-Q_g\propto v$. In the general case $[H,Q]\neq 0$, $\langle Q\rangle-Q_g$ is not necessarily proportional to b^2. However, if the matrix element $\langle\psi_i Q\psi_g\rangle$ is negligible, we obtain

$$\langle Q\rangle - Q_g = -b^2 Q_g + \sum_{ij} b_i b_j\langle\psi_i Q\psi_j\rangle$$
$$= -b^2\left(Q_g - \sum_{ij} b_i b_j\langle\psi_i Q\psi_j\rangle \Big/ \sum_i b_i^2\right). \tag{3.16}$$

This shows that $\langle Q\rangle-Q_g$ is proportional to the variance v. Thus, if $\langle\psi_i Q\psi_g\rangle$ is small, we can perform an extrapolation using a linear fit to obtain the expectation values. We expect that this is the case for short-range correlation functions, since the local correlation may give rise to small effects in the orthogonality of ψ_i and ψ_g, i.e., $\langle\psi_i\psi_g\rangle=0$. Hence the evaluations of local quantities will be much easier than for the long-range correlation functions.

IV. OPTIMIZATION IN QUANTUM MONTE CARLO DIAGONALIZATION

A. Simplest algorithm

The simplest procedure for optimizing the ground-state wave function is to increase the number of basis states $\{\phi_m\}$ by random sampling. First, we set τ and M, for example, $\tau=0.1,0.2,\ldots$, and $M=20,30,\ldots$. We denote the number of basis functions as N_{states}. We start with $N_{states}=100-300$ and then increase up to 2000 or 3000. This procedure can be outlined as follows:

(A1) Generate the auxiliary fields s_i ($i=1,\ldots,N$) in $B_\ell^\sigma(\{s_i\})$ randomly for $\ell=1,\ldots,M$ for ϕ_m ($m=1,\ldots,N_{states}$), and generate N_{states} basis wave function $\{\phi_m\}$.

(A2) Evaluate the matrices $H_{mn}=\langle\phi_m H\phi_n\rangle$ and $A_{mn}=\langle\phi_m\phi_n\rangle$, and diagonalize the matrix $A^{-1}H$ to obtain $\psi=\Sigma_m c_m\phi_m$. Then calculate the expectation values and the energy variance.

(A3) Repeat the procedure from (A1) after increasing the number of basis functions.

For small systems this random method produces reliable energy results. The diagonalization plays an important role in producing fast convergence.

Failure of this simple method sometimes occurs as the system size is increased. The eigenfunction of $A^{-1}H$ can be localized when the off-diagonal elements are small, meaning that some components of c_m are large and others are negligible. A quotient of localization in the configuration space can be defined. For example, the summation of $|c_m|^2$ except ϕ_n with large c_n is a candidate for such property,

$$Q_{loc} = \sum_m{}' |c_m|^2, \tag{4.1}$$

where the prime indicates that the summation is performed excluding the largest c_n. Q_{loc} should approach 1 as the number of basis functions is increased. In the case of localization, $Q_{loc}<0.1$, where to lower the energy is procedurally inefficient. There are two possible procedures to avoid the localization difficulty. First is to multiply ϕ_m by $B_\ell^\sigma(\{s_i\})$ to improve and optimize the basis wave function ϕ_m further. Second, use a more effective method to generate new basis functions, which will be explained further in the subsequent sections.

B. Renormalization

The basis functions $\{\phi_m\}$ multiplied by B_ℓ^σ ($\ell=M+1,M+2,\ldots$) are improved to provide a lower ground state. Here the "improvement" means the increase of τ in Eq. (2.2), which is accomplished by increasing M. The matrix $B_\ell^\sigma(\{s_i\})$ is given by a summation over 2^N configurations of $\{s_i\}$. If we consider all of these configurations, the space required for basis functions becomes large. Thus, we should select sev-

eral configurations or one configuration that exhibits the lowest energy. One procedure to choose such a state is the following:

(B1) Multiply ϕ_m by $\Pi_\sigma \exp(2a\sigma s_j n_{j\sigma} - \frac{1}{2}U\Delta\tau n_{j\sigma})$, where we generate the auxiliary fields $s_i(\ell)$ for $\ell = M+1$ and $i = 1, \ldots, N$ using random numbers. Then evaluate the ground-state energy. If the energy is lower, ϕ_m is defined as a new and improved basis function. If we have a higher energy, ϕ_m remains unchanged. Repeat this procedure to lower the ground-state energy 20–50 times.

(B2) Repeat above for $m = 1, \ldots, N_{states}$.

(B3) Multiply ϕ_m by the kinetic operators $e^{-\Delta\tau K_\uparrow}$ and $e^{-\Delta\tau K_\downarrow}$.

(B4) Repeat from (B1) and continue for $\ell \to \ell + 1$.

This method is referred to as the $1/2^N$ method in this paper, since one configuration is chosen from 2^N possible states. It is important to note that N_{states} remains unchanged. An alternative method has been proposed to renormalize $\{\phi_m\}$ and is outlined as[24] follows:

(B′1) Multiply ϕ_m by $\Pi_\sigma \exp(2a\sigma s_j n_{j\sigma} - \frac{1}{2}U\Delta\tau n_{j\sigma})$ and evaluate the energy for $s_j = 1$ and $s_j = -1$. We adopt s_j for which we have the lower energy.

(B′2) Repeat this procedure for $j = 1, \ldots, N$ and determine the configuration $\{s_j\}$ for ϕ_m.

(B′3) Multiply ϕ_m by the kinetic operators $e^{-\Delta\tau K_\uparrow}$ and $e^{-\Delta\tau K_\downarrow}$.

(B′4) Repeat above for $m = 1, \ldots, N_{states}$ to improve ϕ_m, and repeat from (B1).

In this latter method, the energy is calculated for the auxiliary field $s_i = \pm 1$ at each site before making a selection. In the literature,[24] this procedure is called the path-integral renormalization group (PIRG) method.

C. Genetic algorithm

In order to lower the ground-state energy efficiently, we can employ a genetic algorithm[44] to generate the basis set from the initial basis set. One idea is to replace some parts of $\{s_i(\ell)\}$ $(i = 1, \ldots, N; \ell = 1, \ldots, M)$ in ϕ_n that has the large weight $|c_n|^2$ to generate a different basis function ϕ'_n. The basis function ϕ'_n obtained in this way is expected to also have a large weight and contribute to ψ.

Let us consider two basis functions ϕ_m and ϕ_n chosen from the basis set with a probability proportional to the weight $|c_j|^2$ using uniform random numbers. For example, since $\Sigma_{allj}|c_j|^2 = 1$, we set the weight of ϕ_ℓ to occupy $\Sigma_{j=1}^{\ell-1}|c_j|^2 < x < \Sigma_{j=1}^{\ell}|c_j|^2$ in the range $0 < x < 1$. If the random number r is within $\Sigma_{j=1}^{m-1}|c_j|^2 < r < \Sigma_{j=1}^{m}|c_j|^2$, we choose ϕ_m, and ϕ_n is similarly chosen. A certain part of the genetic data between ϕ_m and ϕ_n is exchanged, which results in two other basis functions ϕ'_m and ϕ'_n. We add ϕ'_n or ϕ'_m, or both of them, to the set of basis functions as elements. In this process, every site is labeled using integers such as $i = 1, \ldots, N$, and then we exchange s_i for $i = L_1, L_1+1, \ldots, L_1+L_{exch}-1$, where the number of s_i to be exchanged is denoted as L_{exch}. L_1 can be determined using random numbers. We must also include a randomly generated basis function as a mutation. Here we fix the numbers N_{states} and N_{step} before starting the Monte Carlo steps. For instance, $N_{states} = 200$ and $N_{step} = 200$.

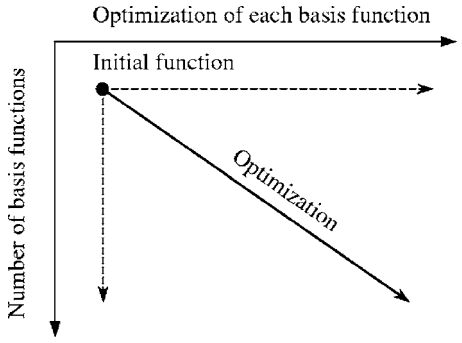

FIG. 1. Concept of optimization procedure. There are three approaches to reach the ground-state wave function. First is to increase the number of basis functions for fixed m. Second is to increase M by multiplying each basis function by $B_\ell(\{s_i\})$. Third is the hybrid method of the previous two procedures.

N_{states} is increased as the Monte Carlo steps progress. We diagonalize the Hamiltonian $A^{-1}H$ at each step when the N_{step} basis functions are added to the basis set in order to recalculate the weight $|c_k|^2$ $(k = 1, 2, \ldots)$. The procedure is summarized as follows:

(C1) Generate the auxiliary fields $s_i(\ell)$ $(i = 1, \ldots, N)$ randomly for $\ell = 1, \ldots, M$. Generate N_{states} basis functions $\{\phi_k\}$. This is the same as (A1).

(C2) Evaluate the matrices $H_{mn} = \langle \phi_m H \phi_n \rangle$ and $A_{mn} = \langle \phi_m \phi_n \rangle$, and diagonalize the matrix $A^{-1}H$ to obtain $\psi = \Sigma_m c_m \phi_m$, then calculate the expectation values and the energy variance. This is the same as (A2).

(C3) Determine whether a different basis function should be generated randomly or using the genetic method on the basis of random numbers. Let r_c be in the range $0 < r_c < 1$, for example, $r_c = 0.9$. If the random number r is less than r_c, a different basis function is defined using the genetic algorithm and the next step (C4) is executed; otherwise, generate the auxiliary fields $\{s_i\}$ randomly and go to (C6).

(C4) The weight of ϕ_k is given as $|c_k|^2$. Choose two basis functions ϕ_m and ϕ_n from the basis set with a probability proportional to the weight $|c_k|^2$. Now we determine which part of the genetic code is exchanged between ϕ_m and ϕ_n. We choose $\ell = \ell_0$ for $1 \leqslant \ell \leqslant M$ using random numbers. We choose the sites $j = L_1, \ldots, L_2 = L_1 + L_{exch} - 1$ for a randomly chosen L_1.

(C5) Exchange the genetic code $\{s_i(\ell)\}$ between ϕ_m and ϕ_n for $\ell = \ell_0$ and $j = L_1, \ldots, L_2 + L_{exch} - 1$. We have two other functions ϕ'_m and ϕ'_n. We adopt one or two of them as basis functions and keep the originals ϕ_m and ϕ_n in the basis set.

(C6) If the N_{step} basis functions are added up to the basis set after step (C2), then repeat from step (C2); otherwise, repeat from step (C3).

D. Hybrid optimization algorithm

In actual calculations it is sometimes better to use a hybrid of genetic algorithm and renormalization method. The concept to reach the ground-state wave function employed in this study is presented in Fig. 1. There are two possible paths: one is to increase the number of basis functions using

the genetic algorithm and the other is to improve each basis function by the matrix $B_\ell(\{s_i\})$. The path followed when the hybrid procedure is employed is the average of these two paths and is represented as the diagonal illustrated in Fig. 1. Before step (C6) in the genetic algorithm, the basis functions ϕ_m are multiplied by $B_\ell(\{s_i\})$ following the renormalization algorithm of steps (B1) to (B3). Then we go to (C6). The method is summarized as follows:

(D1) Generate the auxiliary fields $s_i(\ell)$ $(i=1,\ldots,N)$ randomly for $\ell=1,\ldots,M$. Generate N_{states} basis functions $\{\phi_k\}$.

(D2) Evaluate the matrices $H_{mn}=\langle\phi_m H\phi_n\rangle$ and $A_{mn}=\langle\phi_m\phi_n\rangle$, and diagonalize the matrix $A^{-1}H$ to obtain $\psi=\Sigma_m c_m\phi_m$, then calculate the expectation values and the energy variance.

(D3) Determine whether a different basis should be generated randomly or using the genetic algorithm. Let r_c be in the range $0<r_c<1$. If the random number r is less than r_c, a different basis function is defined using the genetic algorithm and the next step is (D4); otherwise, generate the auxiliary fields $\{s_i\}$ randomly and go to (D6).

(D4) The weight of ϕ_k is given as $|c_k|^2$. Choose two basis functions ϕ_m and ϕ_n from the basis set with a probability proportional to the weight $|c_k|^2$. Now we determine which part of the genetic code is exchanged between ϕ_m and ϕ_n. We choose $\ell=\ell_0$ for $1\leqslant\ell\leqslant M$ using random numbers. We choose the sites $j=L_1,\ldots,L_2=L_1+L_{exch}-1$ for a randomly chosen L_1.

(D5) Exchange the genetic code $\{s_i\}$ between ϕ_m and ϕ_n for $\ell=\ell_0$ and j determined in step (D4). We have two other functions ϕ'_m and ϕ'_n. We adopt one or two of them as basis functions and keep the originals ϕ_m and ϕ_n in the basis set.

(D6) Multiply ϕ_m by $\Pi_\sigma\exp(2a\sigma s_j n_{j\sigma}-\frac{1}{2}U\Delta\tau n_{j\sigma})$, where we generate the auxiliary fields $s_i(\ell)$ for $\ell=M+1$ and $i=1,\ldots,N$ using random numbers. Then evaluate the ground-state energy. If the energy is lower, ϕ_m is defined as an improved basis function. If we have a higher energy, ϕ_m remains unchanged. Repeat this procedure to lower the ground-state energy 20–50 times.

(D7) Repeat above for $m=1,\ldots,N_{states}$.

(D8) Multiply ϕ_m by the kinetic operators $e^{-\Delta\tau K_\uparrow}$ and $e^{-\Delta\tau K_\downarrow}$.

(D9) If the N_{step} basis functions are added up to the basis set after step (D2), then repeat from (D2); otherwise, repeat from step (D3).

E. Discussion on the quantum Monte Carlo diagonalization

The purpose of the QMD method is to calculate

$$\langle Q\rangle=\frac{\sum_{mn}c_m c_n\langle\phi_m Q\phi_n\rangle}{\sum_{mn}c_m c_n\langle\phi_m\phi_n\rangle}. \tag{4.2}$$

In an algorithm based on the quantum Monte Carlo procedures, we evaluate the expectation values in the subspace $\{\phi_i\}$, selected from all the configurations of the auxiliary fields. From the data showing how the mean values $\langle Q\rangle$ vary as the subspace is enlarged, we can estimate the exact value of $\langle Q\rangle$ using an extrapolation. A devised algorithm may help us to perform the quantum Monte Carlo evaluations efficiently. We have presented the genetic algorithm and the renormalization method. It may be possible to overcome the problem of localization in the subspace using this algorithm. In fact, the quotient Q_{loc} in Eq. (4.1) becomes nearly 1, i.e., $Q_{loc}>0.99$, in the evaluations presented in the next section. For such a case, most of the basis functions in the subspace give contributions to the mean values of physical quantities and the obtained results are certainly reliable.

V. RESULTS

In this section, the results obtained using the QMD method are compared to the exact and available results. We investigate the small clusters (such as 4×4 and 6×6), the one-dimensional (1D) Hubbard model, the ladder Hubbard model, and the 2D Hubbard model.

A. Ground-state energy and correlation functions: Check of the method

The results for the 4×4, 6×2, and 6×6 systems are presented in Table I. The results are compared to the exact values and those available values obtained using the exact diagonalization, the quantum Monte Carlo method, the constrained path Monte Carlo method,[22] and the variational Monte Carlo method for lattices with periodic boundary conditions. The expectation values for the ground-state energy are presented for several values of U. The data include the cases for open-shell structures where the highest-occupied energy levels are partially occupied by electrons. In the open-shell cases, the evaluations are sometimes extremely difficult. As is apparent from Table I, our method gives results in reasonable agreement with the exact values. The energy as a function of the variance is presented in Figs. 2–4. To obtain these results, the genetic algorithm was employed to produce the basis functions except the open symbols in Fig. 4. The 4×4 system, where $N_e=10$ in Fig. 2, is the energy for the closed-shell case up to 2000 basis states. The other two figures are for open-shell cases, where evaluations were performed up to 3000 states. Open symbols in Fig. 4 indicate the energy obtained using the renormalization method ($1/2^N$ method) with 300 basis states. The results for the QMD and $1/2^N$ method (or PIRG) are quite similar as a function of the energy variance. In these cases, Q_{loc} is close to 1; $Q_{loc}\sim0.99$. As the variance is reduced, the data can be fitted using a straight line using the least-squares method.

In Table I we have also included the variational Monte Carlo (VMC) results for the λ functions. The λ functions are variational functions defined as follows. The Gutzwiller function is well known as

$$\psi_G=P_G\psi_0, \tag{5.1}$$

where P_G is the Gutzwiller projection operator,

$$P_G=\prod_j[1-(1-g)n_{j\uparrow}n_{j\downarrow}]. \tag{5.2}$$

g is the parameter in the range $0\leqslant g\leqslant1$. The noninteracting wave function ψ_0 is optimized by controlling the double oc-

TABLE I. Ground-state energy per site from the Hubbard model. The boundary conditions are periodic in both directions. The current results are presented under the column labeled QMD. The constrained path Monte Carlo (CPMC) and path-integral renormalization group (PIRG) results are from Refs. 22 and 24, respectively. The column VMC presents the results obtained for the optimized variational wave function $\psi_\lambda^{(2)}$ except for the 6×2 system for which $\psi_\lambda^{(1)}$ is employed. The QMC results are from Ref. 19. Exact results are obtained using diagonalization. (Ref. 45).

Size	N_e	U	QMD	VMC	CPMC	PIRG	QMC	Exact
4×4	10	4	−1.2237	−1.221(1)	−1.2238			−1.2238
4×4	14	4	−0.9836	−0.977(1)	−0.9831			−0.9840
4×4	14	8	−0.732(2)	−0.727(1)	−0.7281			−0.7418
4×4	14	10	−0.656(2)	−0.650(1)				−0.6754
4×4	14	12	−0.610(4)	−0.607(2)	−0.606			−0.6282
6×2	10	2	−1.058(1)	−1.040(1)				−1.05807
6×2	10	4	−0.873(1)	−0.846(1)				−0.8767
6×6	34	4	−0.921(1)	−0.910(2)		−0.920	−0.925	
6×6	36	4	−0.859(2)	−0.844(2)		−0.8589	−0.8608	

cupancy $\Sigma_j\langle n_{j\uparrow}n_{j\downarrow}\rangle$. The further optimization of the Gutzwiller function can be obtained,[48,49]

$$\psi_\lambda^{(1)} = e^{-\lambda K}e^{-\alpha V}\psi_G, \tag{5.3}$$

$$\psi_\lambda^{(2)} = e^{-\lambda' K}e^{-\alpha' V}\psi_\lambda^{(1)}, \tag{5.4}$$

where K is the kinetic-energy term and V is the on-site Coulomb interaction,

$$V = \sum_j n_{j\uparrow}n_{j\downarrow}, \tag{5.5}$$

where λ, α, λ', and α' are variational parameters to be determined to lower the ground-state energy. α is related to g as $\alpha=\log(1/g)$. This type of wave function is referred to as λ function in this paper. In our calculations, the second-level λ function $\psi_\lambda^{(2)}$ has given good results for the ground-state energy. If we perform an extrapolation as a function of the variance, we can obtain the correct expectation values as the QMD method. We must, however, determine variational parameters in the multiparameter space by adjusting the values of the parameters to find a minimum. The advantage of the variational procedure is that the evaluations are stable even for large U/t beyond the bandwidth.

The correlation functions for the 4×4 system, where $N_e=10$ and $U=4$, are presented in Table II. The exact diagonalization results are also provided. The correlation functions are defined as

$$S(\mathbf{q}) = \frac{1}{N}\sum_{ji} e^{i\mathbf{q}\cdot(\mathbf{R}_j-\mathbf{R}_i)}\langle(n_{j\uparrow}-n_{j\downarrow})(n_{i\uparrow}-n_{i\downarrow})\rangle, \tag{5.6}$$

$$C(\mathbf{q}) = \frac{1}{N}\sum_{ji} e^{i\mathbf{q}\cdot(\mathbf{R}_j-\mathbf{R}_i)}(\langle n_j n_i\rangle - \langle n_j\rangle\langle n_i\rangle), \tag{5.7}$$

$$s(i,j) = \langle(n_{j\uparrow}-n_{j\downarrow})(n_{i\uparrow}-n_{i\downarrow})\rangle, \tag{5.8}$$

$$c(i,j) = \langle n_j n_i\rangle - \langle n_j\rangle\langle n_i\rangle, \tag{5.9}$$

where $n_j=n_{j\uparrow}+n_{j\downarrow}$ and $\mathbf{R}_j$ denotes the position of the jth site. $\Delta_{\alpha\beta}$ is the pair-correlation function,

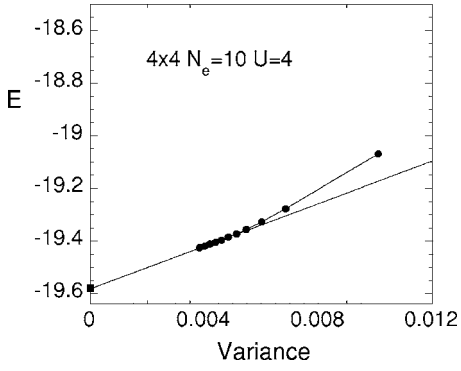

FIG. 2. Energy as a function of the variance for 4×4 system, $U=4$ and $N_e=10$. The square is the exact result. The data are fitted using a straight line using the least-squares method as the variance is reduced. We started with $N_{states}=100$ (first solid circle) and then increased up to 2000.

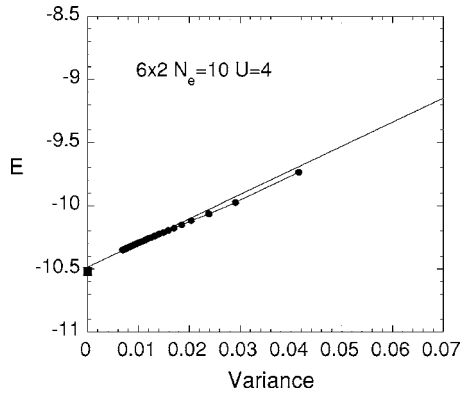

FIG. 3. Energy as a function of the variance for 6×2 $N_e=10$ and $U=4$. The square is the exact value obtained using exact diagonalization.

TABLE II. Correlation functions for the 4×4 Hubbard model with periodic boundary conditions. Parameters are $N_e=10$ and $U=4$. VMC indicates the variational Monte Carlo results obtained by $\psi_\lambda^{(2)}$. CPMC indicates the constrained path Monte Carlo results.

Correlation function	QMD	VMC	CPMC	Exact
$S(\pi,\pi)$	0.730(1)	0.729(2)	0.729	0.7327
$C(\pi,\pi)$	0.508(1)	0.519(2)	0.508	0.5064
$\Delta_{yy}(1)$	0.077(1)	0.076(1)		0.07685
$\Delta_{yy}(2)$	0.006(1)	0.006(1)		0.00624
$\Delta_{xy}(0)$	0.124(1)	0.120(2)		0.1221
$\Delta_{xy}(1)$	−0.015(1)	−0.015(1)		−0.0141
$s(0,0)$	0.529(1)			0.5331
$s(1,0)$	−0.091(1)			−0.0911
$c(0,0)$	0.329(1)			0.3263
$c(1,0)$	−0.0536(1)			−0.05394

$$\Delta_{\alpha\beta}(\ell)=\langle\Delta_\alpha^\dagger(i+\ell)\Delta_\beta(i)\rangle, \tag{5.10}$$

where $\Delta_\alpha(i)$, $\alpha=x,y$, denote the annihilation operators of the singlet electron pairs for the nearest-neighbor sites:

$$\Delta_\alpha(i)=c_{i\downarrow}c_{i+\hat{\alpha}\uparrow}-c_{i\uparrow}c_{i+\hat{\alpha}\downarrow}. \tag{5.11}$$

Here $\hat{\alpha}$ is a unit vector in the $\alpha(=x,y)$ direction. The agreement in this case is good for such a small system. The correlation functions are also dependent on the number of basis wave functions as shown in Fig. 5. Since the fluctuation of the expectation values is small in this case, the extrapolation can be performed in terms of the $1/N_{states}$.

B. 1D and ladder Hubbard models

In this section, we show the results for the 1D Hubbard model and the ladder Hubbard model. The ground state of the 1D Hubbard model is no longer Fermi liquid for $U>0$. The ground state is insulating at half-filling and metallic for less than half-filling. Figure 6 is the spin and charge correlation functions, $S(k)$ and $C(k)$, as a function of the wave number, for the 1D Hubbard model where $N=80$. The $2k_F$ singularity can be clearly identified, where the dotted line is for $U=0$. The spin correlation is enhanced and the charge correlation function is suppressed slightly because of the Coulomb interaction. The momentum distribution function $n(k)$,

$$n(k)=\frac{1}{2}\sum_\sigma\langle c_{k\sigma}^\dagger c_{k\sigma}\rangle, \tag{5.12}$$

is presented in Fig. 7 for the electron filling $n=0.825$. Here $c_{k\sigma}$ is the Fourier transform of $c_{j\sigma}$. $n(k)$ in the metallic phase exhibits a singular behavior near the wave number k_F. The singularity close to k_F is consistent with the property of the Luttinger liquid.[50,51] It is difficult to analyze the singularity in more detail using the Monte Carlo method since there is a sharp decrease at $k=k_F$ as shown in Fig. 7. Note that the Gutzwiller function gives the unphysical result that $n(k)$ increases as k approaches k_F from above the Fermi surface.

In the ladder Hubbard model,

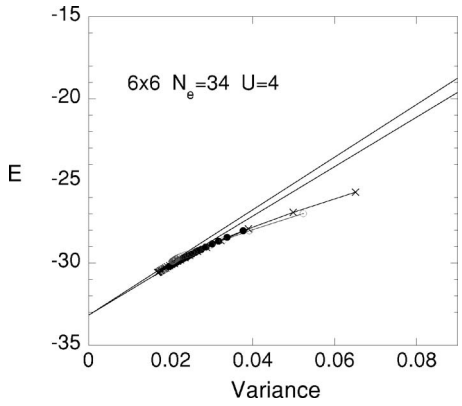

FIG. 4. Energy as a function of the variance v for the 6×6 system with the periodic boundary conditions. Solid circles and crosses are data obtained from the QMD method for two different initial configurations of the auxiliary fields. Gray open circles show results obtained from the $1/2^N$ renormalization method (PIRG) with 300 basis wave functions.

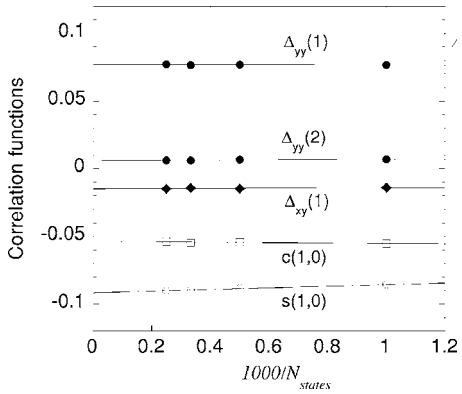

FIG. 5. Correlation functions obtained by QMD for 4×4 lattice with $N_e=10$ and $U=4$ as a function of $1/N_{states}$.

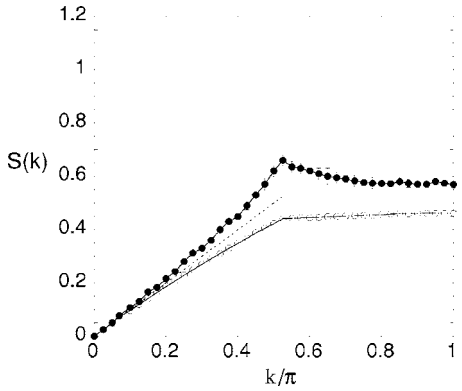

FIG. 6. Spin (solid circle) and charge (open circle) correlation functions obtained from the QMD method for the one-dimensional Hubbard model with 80 sites. The number of electrons is 66. We set $U=4$ and use the periodic boundary condition.

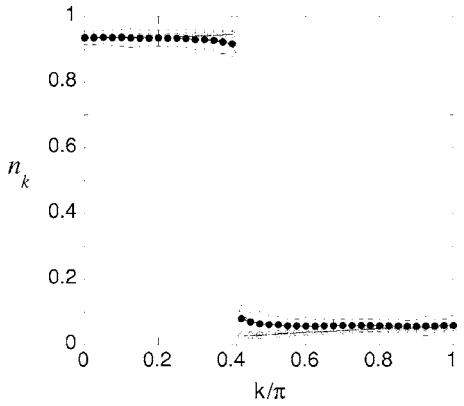

FIG. 7. Momentum distribution function obtained from the QMD method for the one-dimensional Hubbard model with 80 sites for the periodic boundary condition. The number of electrons is 66 and the Coulomb repulsion is $U=4$. The dotted line is the guide given by $n_k \sim 0.5+0.4|k-k_F|^{\eta-1}$, where $\eta-1 \sim 0.035$, which corresponds to $K_\rho \sim 0.69$ using the formula $\eta-1=(K_\rho+K_\rho^{-1})/4-1/2$ (Ref. 50). Open circles are the results obtained using the Gutzwiller function.

$$H_{ladder} = -t \sum_{\ell=1,2} \sum_{j\sigma} (c^\dagger_{\ell j\sigma} c_{\ell j+1,\sigma} + \text{H.c.}) - t_d \sum_{j\sigma} (c^\dagger_{1j\sigma} c_{2j\sigma} + \text{H.c.}) + U \sum_{\ell=1,2} \sum_{j} c^\dagger_{\ell j\uparrow} c_{\ell j\uparrow} c^\dagger_{\ell j\downarrow} c_{\ell j\downarrow}, \tag{5.13}$$

where t (t_d) is the intrachain (interchain) transfer energy. The ladder Hubbard model exhibits a spin gap at half-filling, and the charge gap is also possibly opened for large $U>0$ at half-filling. The existence of a superconducting phase has been suggested for the Hubbard ladder using the density-matrix renormalization group (DMRG) method[38] and the VMC method.[36]

The spin-correlation function $S(\mathbf{k})$ for the Hubbard ladder is presented in Fig. 8, where $U=4$ and $t_d=1$. $S(\mathbf{k})$ is defined as

$$S(\mathbf{k}) = \frac{1}{N} \sum_{i\ell,j\ell'} e^{i\mathbf{k}\cdot(\mathbf{R}_{i\ell}-\mathbf{R}_{j\ell'})} \langle (n_{\ell i\uparrow} - n_{\ell i\downarrow})(n_{\ell' j\uparrow} - n_{\ell' j\downarrow}) \rangle, \tag{5.14}$$

where $\mathbf{R}_{i\ell}$ denotes the site (i,ℓ) $(\ell=1,2)$. We use the convention that $\mathbf{k}=(k,k_y)$, where $k_y=0$ and π indicate the lower band and upper band, respectively. There are four singularities at $2k_{F1}$, $2k_{F2}$, $k_{F1}-k_{F2}$, and $k_{F1}+k_{F2}$ for the Hubbard ladder, where k_{F1} and k_{F2} are the Fermi wave numbers of the lower and upper bands, respectively. They can be clearly identified as indicated by arrows in Fig. 8.

The momentum distribution in Fig. 9,

$$n(\mathbf{k}) = \frac{1}{2N} \sum_{\sigma} \sum_{i\ell,j\ell'} e^{i\mathbf{k}\cdot(\mathbf{R}_{i\ell}-\mathbf{R}_{j\ell'})} \langle c^\dagger_{\ell i\sigma} c_{\ell' j\sigma} \rangle, \tag{5.15}$$

exhibits singularities at k_{F1} and k_{F2}, where the results obtained from the Gutzwiller function are also shown for comparison. Here, we used the same notation for $\mathbf{k}$ and $\mathbf{R}_{i\ell}$. The unphysical property of $n(\mathbf{k})$ near the Fermi wave numbers for the Gutzwiller function are remedied in the QMD method.

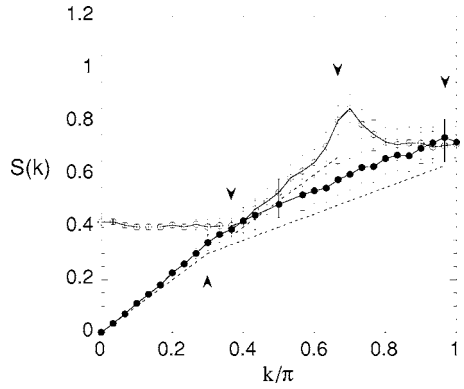

FIG. 8. Spin-correlation function obtained from the QMD method for the ladder Hubbard model for 60×2 sites with periodic boundary condition. The number of electrons is 80 and $U=4$. The upper line is for the upper band and the lower line is for the lower band. Singularities are at $k_{F1}-k_{F2}$, $2k_{F2}$, $k_{F1}+k_{F2}$, and $2k_{F1}$ from left. The dotted lines are for $U=0$.

The pair-correlation function, $\Delta_{yy}(\ell)$ versus ℓ, was also evaluated to compare with the DMRG method. $\Delta_{yy}(\ell)$ is defined as

$$\Delta_{yy}(\ell) = \langle \Delta^\dagger_y(i+\ell) \Delta_y(i) \rangle \tag{5.16}$$

for

$$\Delta_y(i) = c_{1i\downarrow} c_{2i\uparrow} - c_{1i\uparrow} c_{2i\downarrow}. \tag{5.17}$$

$\Delta_{yy}(\ell)$ is the correlation function for the singlet pair on the rung. The results for $\Delta_{yy}(\ell)$ are given in Fig. 10 on the 16×2 lattice for the open boundary condition, where the pair-correlation functions $\Delta_{yy}(\ell)$ were averaged over several pairs for a distance ℓ. The values $U=4$ and $t_d=1.4$ are predefined, and the electron filling was $n=0.875$. The result obtained using the DMRG method is also provided for $U=8$ (Ref. 38)

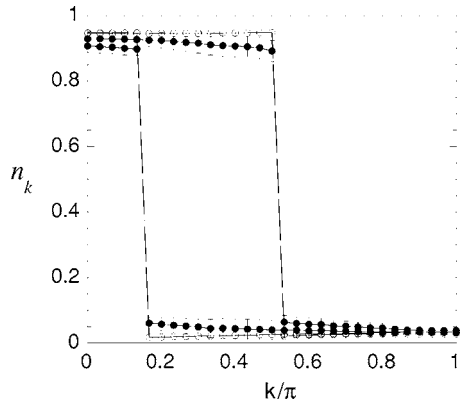

FIG. 9. Momentum distribution function obtained from the QMD method for the ladder Hubbard model for 60×2 sites and periodic boundary condition. The number of electrons is 80 and $U=4$.

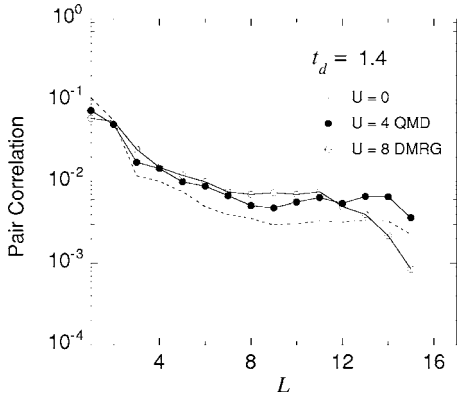

FIG. 10. Pair-correlation function (solid circles) obtained using the QMD method for the ladder Hubbard model with 16×2 sites, where the boundary condition is open. $U=4$, $t_d=1.4$, and the electron filling is 0.875. The dashed line is the pair-correlation function for $U=0$. The open circles are the DMRG results from Ref. 38.

for comparison. Since a large value of U, such as $U=8$, is not easily accessed using the QMD method, we have presented the results for $U=4$. The enhancement of the pair-correlation function over the noninteracting case is clear and is consistent with the DMRG method.

It has been expected that the charge gap opens up as U turns on at half-filling for the Hubbard ladder model. In Fig. 11 the charge gap at half-filling is shown as a function of U. The charge gap is defined as

$$\Delta_c = E(N_e+2) + E(N_e-2) - 2E(N_e), \tag{5.18}$$

where $E(N_e)$ is the ground-state energy for the N_e electrons. The charge gap in Fig. 11 was estimated using the extrapolation to the infinite system from the data for the 20×2, 30×2, and 40×2 systems. The data are consistent with the DMRG method and suggest the exponentially small charge gap for small U or the existence of the critical value U_c in the range of $0\leqslant U_c<1.5$, below which the charge gap vanishes.

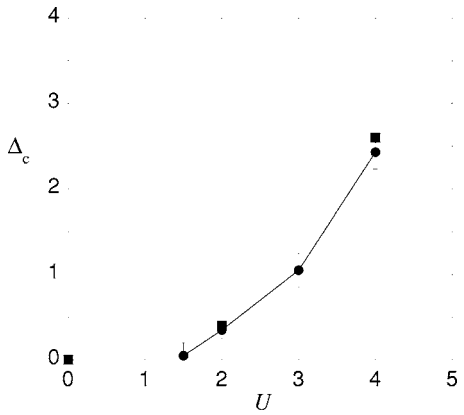

FIG. 11. Charge gap as a function of U for $t_d=1$ (circles). The DMRG results (squares) are provided for comparison (Ref. 40).

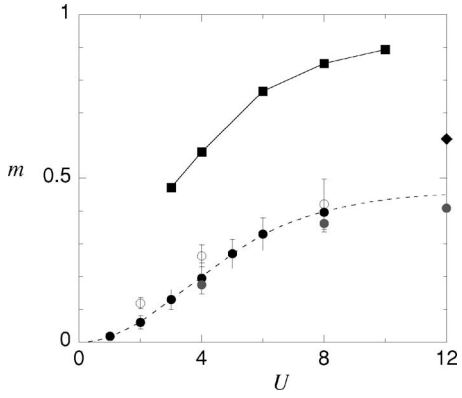

FIG. 12. Magnetization as a function of U for the half-filled Hubbard model after extrapolation at the limit of large N. Solid circles are the QMD results and open circles are results obtained from the QMC method (Ref. 12). The squares are the Gutzwiller-VMC results (Ref. 25) and gray solid circles show the third λ function ($\psi_\lambda^{(3)}$) VMC results carried out on the 8×8 lattice (Ref. 49). The diamond symbol is the value from the two-dimensional Heisenberg model, where $m=0.615$ (Refs. 46 and 47).

C. 2D Hubbard model

The two-dimensional Hubbard model was also investigated in this study. The results are presented in the following discussion. An important issue is the antiferromagnetism at half-filling. The ground state is antiferromagnetic for $U>0$ because of the nesting due to the commensurate vector $Q=(\pi,\pi)$. The Gutzwiller function predicts that the magnetization

$$m = \left| \frac{1}{N}\sum_j (n_{j\uparrow} - n_{j\downarrow}) e^{iQ\cdot R_j} \right| \tag{5.19}$$

increases rapidly as U increases and approaches $m=1$ for large U. In Fig. 12, the QMD results are presented for m as a function of U. The previous results obtained using the QMC method are plotted as open circles. The gray circles are for the λ function VMC method and the squares are for the Gutzwiller VMC data. Clearly, the magnetization is reduced considerably because of the fluctuations, and is smaller than the Gutzwiller VMC method by about 50%.

Figure 13 is the momentum distribution function $n(\mathbf{k})$,

$$n(\mathbf{k}) = \frac{1}{2}\sum_\sigma \langle c^\dagger_{\mathbf{k}\sigma} c_{\mathbf{k}\sigma}\rangle, \tag{5.20}$$

where the results for the Gutzwiller VMC and the QMD are indicated. The Gutzwiller function gives the results that $n(k)$ increases as k approaches k_F from above the Fermi surface. This is clearly unphysical. This flaw of the Gutzwiller function near the Fermi surface is not observed for the QMD result.

VI. SUMMARY

We have presented a quantum Monte Carlo diagonalization method for a many-fermion system. We employ the Hubbard-Stratonovich transformation to decompose the in-

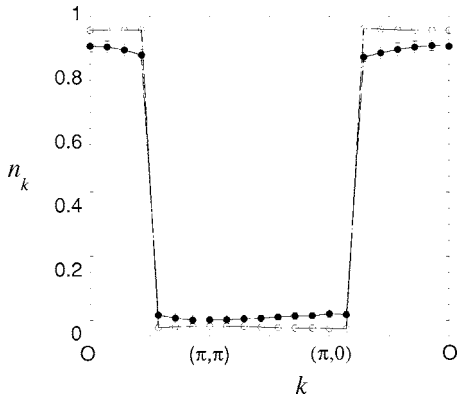

FIG. 13. Momentum distribution function for the 14×14 lattice. Parameters are $U=4$ and $N_e=146$. The boundary conditions are periodic in both directions. The results for the Gutzwiller function (open circle) are also provided.

teraction term as in the standard QMC method. We use this in an expansion of the true ground-state wave function. We have considered the truncated space of the basis functions $\{\phi_m\}$ and diagonalize the Hamiltonian in this subspace. We can optimize the wave function by enlarging the subspace. The simplest way is to increase the number of basis functions by randomly generating auxiliary fields $\{s_i\}$. The wave function can be further improved by multiplying each ϕ_m by B_ℓ^σ. Although the matrix B_ℓ^σ in Eq. (2.6) generates 2^N basis functions, we must select some states from them to keep the number of basis functions small. Within the subspace with the fixed number of basis functions, an extension of the $1/2^N$ method to the $k/2^N$ method ($k=1,2,\ldots$) is also possible.

We have proposed a genetic-algorithm-based method to generate the basis wave functions. The genetic algorithm is widely used in solving problems to find the optimized solution in the space of large configuration numbers. We make other basis functions from the functions with large weighting factors $|c_n|^2$. Functions produced in this way are expected to have large weighting factors. If the localization quotient Q_{loc} in Eq. (4.1) is not small, we can iterate the Monte Carlo steps without using the $1/2^N$ method.

We have computed the energy and correlation functions for small lattices to compare with published data. The results obtained in this study are consistent with the published data. In the case of the open-shell structures, evaluations are difficult in general and the convergence is not monotonic. In this case, the subspace of the basis functions must be large to obtain the expectation values from the extrapolation procedure.

As for the extrapolation, the expectation value $\langle Q\rangle$ may approach Q_{exact} in a nonlinear way,

$$\langle Q\rangle - Q_{exact} \propto (N_{states})^{-\theta} \tag{6.1}$$

for some exponent θ. We must evaluate θ to obtain Q_{exact} from an extrapolation in terms of the N_{states}^{-1}. We may be able to use a derivative method where θ is determined so that the derivative $d\langle Q\rangle/dN_{states}$ approaches 0 as N_{states} increases. In this paper, we adopted the recently proposed energy-variance method.[24,43] For the energy and local quantities, we can expect $\langle Q\rangle - Q_{exact} \propto v$ for the variance v. It is expected that the long-range correlations are not trivial to calculate since the orthogonality $\langle \psi_i Q \psi_g\rangle \approx 0$ should hold for the ground state ψ_g and excited states ψ_i.

ACKNOWLEDGMENTS

We thank J. Kondo, K. Yamaji, and S. Koikegami for helpful discussions.

[1] E. Dagotto, Rev. Mod. Phys. **66**, 763 (1994).
[2] D. J. Scalapino, in *High Temperature Superconductivity—The Los Alamos Symposium 1989 Proceedings*, edited by K. S. Bedell, D. Coffey, D. E. Deltzer, D. Pines, and J. R. Schrieffer (Addison-Wesley, Redwood City, 1990), p. 314.
[3] P. W. Anderson, *The Theory of Superconductivity in the High-T_c Cuprates* (Princeton University Press, Princeton, 1997).
[4] T. Moriya and K. Ueda, Adv. Phys. **49**, 555 (2000).
[5] G. R. Stewart, Rev. Mod. Phys. **56**, 755 (1984).
[6] P. A. Lee, T. M. Rice, J. W. Serene, L. J. Sham, and J. W. Wilkins, Comments Condens. Matter Phys. **12**, 99 (1986).
[7] H. R. Ott, Prog. Low Temp. Phys. **11**, 215 (1987).
[8] M. B. Maple, *Handbook on the Physics and Chemistry of Rare Earths* (North-Holland, Amsterdam, 2000), Vol. 30.
[9] T. Ishiguro, K. Yamaji, and G. Saito, *Organic Superconductors* (Springer-Verlag, Berlin, 1998).
[10] J. Hubbard, Proc. R. Soc. London, Ser. A **276**, 238 (1963).
[11] J. E. Hirsch, Phys. Rev. Lett. **51**, 1900 (1983).
[12] J. E. Hirsch, Phys. Rev. B **31**, 4403 (1985).
[13] S. Sorella, E. Tosatti, S. Baroni, R. Car, and M. Parrinello, Int. J. Mod. Phys. B **2**, 993 (1988).
[14] S. R. White, D. J. Scalapino, R. L. Sugar, E. Y. Loh, J. E. Gubernatis, and R. T. Scalettar, Phys. Rev. B **40**, 506 (1989).
[15] M. Imada and Y. Hatsugai, J. Phys. Soc. Jpn. **58**, 3752 (1989).
[16] S. Sorella, S. Baroni, R. Car, and M. Parrinello, Europhys. Lett. **8**, 663 (1989).
[17] E. Y. Loh, J. E. Gubernatis, R. T. Scalettar, S. R. White, D. J. Scalapino, and R. L. Sugar, Phys. Rev. B **41**, 9301 (1990).
[18] A. Moreo, D. J. Scalapino, and E. Dagotto, Phys. Rev. B **43**, 11442 (1991).
[19] N. Furukawa and M. Imada, J. Phys. Soc. Jpn. **61**, 3331 (1992).
[20] A. Moreo, Phys. Rev. B **45**, 5059 (1992).
[21] S. Fahy and D. R. Hamann, Phys. Rev. B **43**, 765 (1991).
[22] S. Zhang, J. Carlson, and J. E. Gubernatis, Phys. Rev. B **55**, 7464 (1997).
[23] S. Zhang, J. Carlson, and J. E. Gubernatis, Phys. Rev. Lett. **78**, 4486 (1997).
[24] T. Kashima and M. Imada, J. Phys. Soc. Jpn. **70**, 2287 (2001).
[25] H. Yokoyama and H. Shiba, J. Phys. Soc. Jpn. **56**, 1490 (1987); **56**, 3582 (1987).
[26] C. Gros, R. Joynt, and T. M. Rice, Phys. Rev. B **36**, 381 (1987).
[27] T. Nakanishi, K. Yamaji, and T. Yanagisawa, J. Phys. Soc. Jpn.

66, 294 (1997).
[28] K. Yamaji, T. Yanagisawa, T. Nakanishi, and S. Koike, Physica C **304**, 225 (1998).
[29] T. Yanagisawa, S. Koike, and K. Yamaji, Phys. Rev. B **64**, 184509 (2001).
[30] T. Yanagisawa, S. Koike, and K. Yamaji, J. Phys.: Condens. Matter **14**, 21 (2002).
[31] T. Yanagisawa, M. Miyazaki, S. Koikegami, S. Koike, and K. Yamaji, Phys. Rev. B **67**, 132408 (2003).
[32] T. Yanagisawa, M. Miyazaki, and K. Yamaji, J. Phys. Soc. Jpn. **74**, 835 (2005).
[33] M. Miyazaki, K. Yamaji, and T. Yanagisawa, J. Phys. Soc. Jpn. **73**, 1643 (2004).
[34] K. Yamaji and Y. Shimoi, Physica C **222**, 349 (1994).
[35] K. Yamaji, Y. Shimoi, and T. Yanagisawa, Physica C **235-240**, 2221 (1994).
[36] S. Koike, K. Yamaji, and T. Yanagisawa, J. Phys. Soc. Jpn. **68**, 1657 (1999); **69**, 2199 (2000).
[37] R. M. Noack, S. R. White, and D. J. Scalapino, Physica C **270**, 281 (1996).
[38] R. M. Noack, N. Bulut, D. J. Scalapino, and M. G. Zacher, Phys. Rev. B **56**, 7162 (1997).
[39] K. Kuroki, T. Kimura, and H. Aoki, Phys. Rev. B **54**, R15641 (1996).
[40] S. Daul and D. J. Scalapino, Phys. Rev. B **62**, 8658 (2000).
[41] K. Sano, Y. Ono, and Y. Yamada, J. Phys. Soc. Jpn. **74**, 2885 (2005).
[42] R. Blankenbecler, D. J. Scalapino, and R. L. Sugar, Phys. Rev. D **24**, 2278 (1981).
[43] S. Sorella, Phys. Rev. B **64**, 024512 (2001).
[44] D. E. Goldberg, *Genetic Algorithms in Search, Optimization and Machine Learning* (Addison-Wesley, Boston, 1989).
[45] A. Parola, S. Sorella, S. Baroni, R. Car, M. Parrinello, and E. Tosatti, Physica C **162-164**, 771 (1989).
[46] J. A. Riera and A. P. Young, Phys. Rev. B **39**, 9697 (1989).
[47] M. Calandra Buonaura and S. Sorella, Phys. Rev. B **57**, 11446 (1998).
[48] H. Ohtsuka, J. Phys. Soc. Jpn. **61**, 1645 (1992).
[49] T. Yanagisawa, S. Koike, and K. Yamaji, J. Phys. Soc. Jpn. **67**, 3867 (1998); **68**, 3608 (1999).
[50] H. J. Schulz, Int. J. Mod. Phys. B **5**, 57 (1991).
[51] N. Kawakami and S.-K. Yang, Phys. Lett. A **148**, 359 (1990).